Summer 6-27-2014

Evaporation from a capillary tube: Experiment and modelization

Emmanuel Keita
Université Paris-Est, Laboratoire Navier

Pamela Faure
Université Paris-Est, Laboratoire Navier

stephane Rodts
Université Paris-Est, Laboratoire Navier

Phillippe Coussot
Université Paris-Est, Laboratoire Navier

David Weitz
University of Cambridge

Follow this and additional works at: http://dc.engconfintl.org/porous_media_V

Part of the Materials Science and Engineering Commons

EVAPORATION FROM A CAPILLARY TUBE: EXPERIMENT AND MODELISATION

Emmanuel Keita, Paméla Faure, Stéphane Rodts and Philippe Coussot
Université Paris-Est, Laboratoire Navier, Champs sur Marne, 77420, France

David A. Weitz
Department of Physics, Harvard University, Cambridge, Massachusetts, 02138, USA

keita.emmanuel@gmail.com

ABSTRACT
Drying is known to play a major role in soils and buildings materials. Better understanding the physics may help saving cost and energy. Thus control of the drying kinetics is a key factor.

In permeable porous media, capillary forces lead to constant curvature of the air/water interface. The value of the curvature and the shape of the interface depend strongly on the pore geometry. Thus small change in their shape may lead to main change of the air/water interface as the medium desaturates. As the surface is supplied with water the drying rate remains at a constant value set by the area of air/water interface close to the surface.

A capillary tube of rectangular cross section maintains water layers in its 4 corners and reproduce well the drying regimes of a porous medium. Here we show that a small variation in the shape of the cross section modify drastically the invasion of air due to equilibrium of capillary forces. Moreover not only the corners but a large part of the cross section remains wet in particular at the entrance of the tube allowing a high drying rate.

Pore distribution and the opacity of samples make it difficult to locate water and estimate capillary forces with accuracy. Using a simple geometry, we can observe the water distribution and measure the shape of the air/water interface with good resolution in imaging and in time. We observe that the drying rate is constant during the main period of the desaturation even if the air/water interface increases by a factor 10. Using 2D finite element method (FEM), we show that the air inside a large portion of the capillary tube is saturate with water vapor ; thus only a small part of the interface close to the entrance participate to the evaporation flux. More generally we can infer that below one pore diameter air is saturated and the air/water interface does not contribute to drying. The three basic regimes of drying kinetics in porous media assumes that the drying rate will decrease as the capillary forces are no longer able to provide water to the evaporation surface.

In our tube, as desaturation goes further, the drying rate decreases even if the capillary flow still supply water to the surface. Again using FEM, we show that as the wetting surface at the entrance decreases the drying rate will decrease even if no receding front progress. In this situation, the air/water interface inside the tube contributing to the drying increase progressively but this is not enough to maintain the initial high rate.

Interpreting only the water mass loss as a function of time, we may lead to wrong conclusions considering basics drying regimes. In Porous media with the same porosity and a slight variation in pore shape drying rate may differ by order of magnitude. Our understanding of the drying kinetics of a simple geometry opens way to control the pore distribution to tune the drying rate of porous media in situation where capillary effects are dominant.

INTRODUCTION
Put Many industrial processes involve materials containing water which eventually has to be removed. Drying is a required step which is generally strongly energy-consuming. Moreover, controlling drying kinetics is a key factor in soils for agriculture, food conditioning, building materials, paint and others coatings. A better understanding of the physics of this phenomenon may help improving processes and decreasing the cost.

When gravity effects are negligible with regards to capillary effects (typically if $\rho g \ll \gamma/e$), whatever the complexity of the material structure (from simple bead packings to soils) two main stages of drying are observed for an initially saturated permeable medium [1,2,6,7]. The basic physical origin of these regimes is generally assumed to be as follows:

(i) The initial stage, i.e. the so-called Constant Rate Period (CRP), corresponds to a situation for which the capillary pressure acts like a strong pump supplying water to the free surface of the sample where evaporation occurs at a rate set by external conditions (air flow, temperature, hygrometry).

(ii) The second stage, Falling Rate Period (FRP), occurs when the saturation is sufficiently small so that the permeability is too low to allow the liquid to feed the free surface of the sample at the rate of evaporation governed by external conditions. A drying front appears and penetrates the sample, and water vapor has to diffuse from this front through the dry region of the porous system, which explains that the rate of evaporation significantly decreases in time.

The observation of local water saturation and dynamics of the air/water interface inside porous media remains a challenge even with the help of sophisticated tools (MRI, confocal microscopy) in model systems (granular packings). Existing observations tend to confirm that when a dry front develops the drying rate decreases [3-5]. Some knowledge exist concerning the role of wetting of the porous media by the fluid but nothing concerning the impact of the shape of the liquid-air interface on the drying rate. More precise observations are nevertheless possible in ultra-model porous media, i.e. capillary tubes, which thus appear to be a powerful means for an in-depth understanding of the drying behavior of porous systems. In particular it was shown that a capillary tube reproduces the main regimes of drying of porous media [1, 8]. In these works a constant drying rate was associated with the penetration of a finger of air through the tube while liquid flows along the corners, and the subsequent decrease of the drying rate was associated with a depinning of the liquid film from the tube exit as a result of competition between gravity and viscous effects.

Here we observe that in a simple capillary geometry with negligible gravity effects the rate of drying can significantly decrease (by a factor ten) without any receding dry front. With the help of 2D finite element method (FEM) we show that this effect is due to the shape of the liquid-air interface around the free surface of the sample which has a dramatic impact on the rate of evaporation. This finally demonstrates that there exist situations in which there is no receding front in the Falling Rate Period. This suggests that the drying rate of a more complex porous medium can be tuned through the exact pore shape distribution at the free surface even in regimes where capillary effects are dominant.

1 Capillary re-equilibration

We used glass capillary tubes with rectangular section (2 x 0.1 x 10 mm^3). When such a tube is put in contact with water, the liquid saturates it as a result of capillary effects. Once saturated with water the tube was clogged at an extremity with epoxy glue.

Before commenting on the drying process itself, it is important to remark that the channel section was not perfectly rectangular. As appears from SEM images the spacing is larger (e_{max} = 115 µm) in the center and narrower (e_{min} = 95 µm) at the edges approximately with a parabolic shape. This means that the motion of an interface towards the sides of a tube is associated with an increase of the partial curvature (normal to j see Fig. 1. b.) which can be adjusted by the second curvature (normal to i) or leads to an increase of the Laplace pressure drop through the interface.
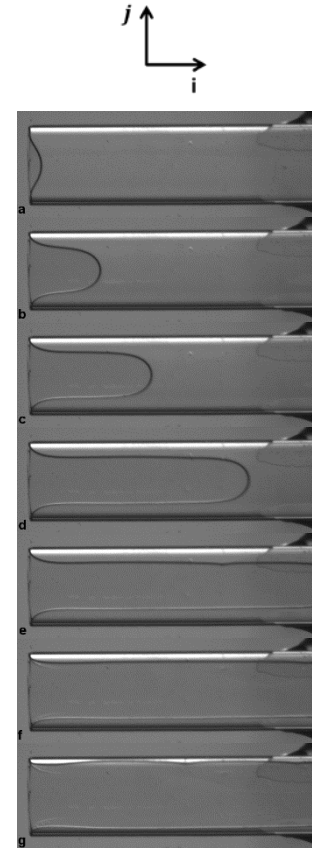
Figure 1: Views from upper of the channel (open on the left) at different times during drying: (a) initial and after 17 (b), 34 (c), 68 (d), 103 (e), 137 (f) and 163 min. (g).

At the beginning of the drying the capillary tube is fully saturated with water so that evaporation occurs from the free surface of the system. Then the air/water interface curves towards the interior of the tube, while water remains at the free surface at both edges (see Fig. 1a). As desaturation goes further, the air forms a finger progressing in the capillary tube (see Fig. 1b). From that point the fingertip keeps a constant shape (approximately a half-circle of radius R =0.6 mm) and progresses with a constant speed leaving water layers of constant thickness h_0=0.4 mm behind it along the tube edges (see Fig.1 c,d). During this period, in a cross-section behind the fingertip, air occupies 60% of the volume. Therefore the total saturation in the tube is 40% when the fingertip reaches the end of the capillary tube. After that the two water layers along the channel axis disconnect at the end and decrease homogenously in thickness until the very late stage of the drying (see Fig.1 d,e), in the limit of the camera resolution.

Since capillary pressure plays a critical role in drying of porous media it is interesting to first study the

distribution and evolution of the curvature of the air-water interface in time. Let us focus on the period of constant fingertip shape. The curvature of the interface in the plane of observation is determined from the images (Fig. 1.d) and the curvature in the orthogonal plane can be inferred from the spacing of the capillary. At the fingertip the total curvature ($1/R$) is approximately $2/e_{max} + 1/R \approx 19 \, \text{mm}^{-1}$; along the straight part of the finger the interface is 0.4 mm from the edge, so that the spacing (e) is equal to 105 µm (see fig 1.b) and the total curvature is $2/e \approx 19 \, \text{mm}^{-1}$; finally using as a first approximate h as radius of curvature (but in a convex shape) in the plane of observation and the minimum spacing (along the edge) we find $2/e_{min} - 1/h \approx 18.5 \, \text{mm}^{-1}$ for the total curvature at the free surface. These results show that the capillary equilibrium is maintained everywhere in the fluid.

This situation persists up to the time when the fingertip reaches the end of the tube, the total curvature is thus constant and uniform during all that period. This means that the liquid has at any time and everywhere a unique Laplace pressure drop with air pressure. Thus capillary forces govern the shape of the interface. Since this situation is similar to that assumed during the CRP in porous media we expect the drying rate to be constant until the very late desaturation when permeability in the *remaining films is too low to pump water to the surface and a drying front progresses.*

The capillary pumping limit can be estimated as follows. When the liquid flow is governed by capillary effects the motion typically results from a pressure gradient of the order of γ/e (where γ is the surface tension) applied to a liquid channel of cross-section eh. We find the velocity from a balance between the capillary pressure and viscous stress, which gives $V_{cap} \approx e\gamma/(\mu L)$ when $h > e$, from which we find $V_{cap} \approx 9.10^{-1} \, \text{m.s}^{-1}$, but when $h < e$ we rather have $V_{cap} \approx h^2 \gamma/(eL\mu)$. On another side the drying rate may be expressed as a velocity: $V_{drying} = (1/S\rho)\text{d}m/\text{d}t \approx 7.10^{-7} \, \text{m.s}^{-1}$, with m the water mass and S the cross section area. Thus we see that during most of the process the capillary velocity will be much larger than the drying velocity, which means that capillary effects are able to supply water immediately when some water volume is removed from the free surface of the sample. A regime change can occur when V_{cap} becomes of the same order as V_{drying}, which occurs for very small values of e, typically of the order of $10^{-7} \, \text{m}$, corresponding to a saturation of the order of 10^{-4}.

2 Constant Rate Period
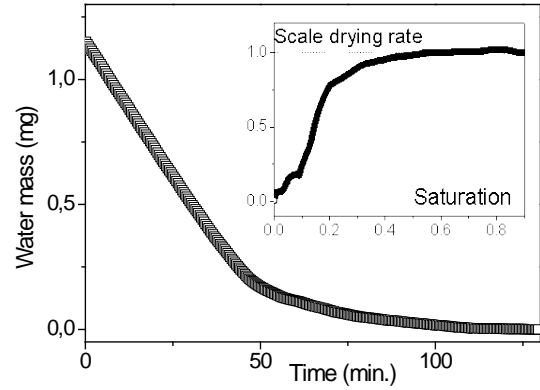
Figure 2: Water mass in capillary tube vs time of drying. Inset shows the scaled drying rate as a function of the saturation.

According to the above calculations we should have an immediate supply of water towards the free surface, leading a priori to a constant drying rate imposed by the external conditions. This is not the case, actually the loss mass curve as a function of time shows that the drying rate is constant down to a saturation (water to available volume ratio) of 0.4, then it significantly decreases while there is still a continuous film along the channel. From a saturation of 0.4 to 0.2 the drying rate slowly decreases, then sharply until 0.1. Such variations are similar to those typically obtained in porous media [2] although the value of the critical saturation slightly varies with the system (for a bead packing it is around 0.1). In our case, at the critical saturation the interface is still with constant curvature which is a sign that capillary effects are still dominant. Moreover the tube remains wetted up to its exit until the very end of the drying (saturation of 0.01).

Thus we observe a strong decrease of the drying rate in a model porous medium in an unexpected configuration. The drying rate decreases whereas the usual conditions for the CRP are still fulfilled, namely capillary effects able to pump the liquid from the porous medium up to the exit and a continuous film covering the solid surfaces throughout the sample.

3 Premature Falling Rate Period
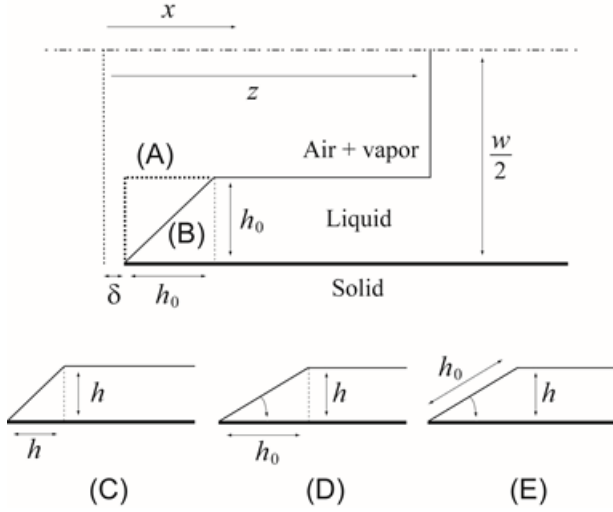
Figure 3: (top) Scheme of half the channel seen from upper and the liquid-air interface assumed in case (A) (dotted line around the entrance) and (B) (continuous line) assumed in the numerical simulations for the period of constant film thickness. (bottom) Different shapes (see text) assumed for the period of decreasing thickness.

In order to understand this effect we model the water vapor field in the tube with the help of 2D Finite Elements Method (FEM). Here we neglect variations in the third dimension, which seems reasonable considering that the length scale in that direction is much smaller (100 µm) than in the two other directions (respectively 2 and 8 mm), and we also neglect the impact, on the drying rate for a given shape of the liquid-air interface, of small thickness variations in the direction z, by considering the tube cross section as rectangular. We will only consider here the case when the finger is already formed. For a straightforward analysis of the results we represent the interface shape by broken lines mainly characterized by two parameters: h the thickness of the water layers and z the length of the air finger (as shown on Fig. 3). First we look at the evolution of the drying rate as it progresses steadily ($h = h_0 = 0.4 \, \text{mm}$) and consider two possible shapes of the film at the entrance (see Fig 3.b): (A) constant film thickness; (B) linear transition from thickness 0 to h_0 over a distance h_0.

We compute the vapor density distribution (n) associated with the interface shape at a given time assuming steady state diffusion and neglecting displacements of the interface induced by vapor flux. Such a description is justified by the fact that the diffusion velocity (of the order of $0.1 \, \text{m.s}^{-1}$) is much larger that the drying velocity. As a consequence the Laplace equation ($\Delta n = 0$) captures the spatial field of vapor saturation. The boundary conditions are: n is equal to the saturation vapor density $n_0 = 23.4 \, \text{g.m}^{-3}$ along the liquid-air interface; we represent the effect of air flow along the exit as a region of rapid variation of

the vapor density (down to $n = n_0/2$ along the outer surface of Ω) over a distance δ from the channel entrance, and we assume that along this region $\nabla n \cdot \mathbf{s} = 0$ (along the lateral outer interface) where $\mathbf{s}$ is the normal vector. This diffusion length (δ) is determined by fitting the drying rate during the initial stage of drying to that measured in our tests (after the air finger has just formed). We found $\delta = 0.094 \, \text{mm}$ in the case (A) and $\delta = 0.0073 \, \text{mm}$ in the case (B).
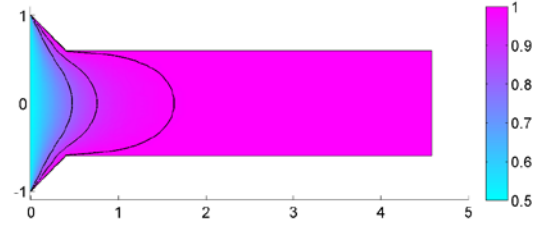
Figure 4: Relative humidity (n/n_0) field as computed from simulations (represented here in terms of reduced relative humidity: $2n/n_0 - 1$) for the geometry (A) when z = 4.6 mm. The lines correspond to isovalues for the relative humidity: (from left to right) 50% (vertical line), 80, 90 and 99%.

A typical vapor density field is shown in Figure 4. It appears that the vapor saturation is reached beyond a short distance from the entrance, of the order of the channel width. Our simulations show that his trend does not change when the finger penetrates farther in the channel so that the impact of the increase of the liquid-air interface on the drying characteristics is questionable. In order to better appreciate it we can compute the vapor flux through the section situated at a distance x in the channel, which is equal to

$$F(x) = -D \int_{x=x_0} \nabla n \cdot d\mathbf{s},$$

where $D = 2.7 \, 10^{-5} \, \text{m}^2.\text{s}^{-1}$ is the diffusion coefficient of water in air. $F(x)$ corresponds to the contribution to the drying rate of the air/water interface beyond x, and $J = F(0)$ is the total drying rate from the sample.

The first important observation is that for both geometries (A and B) J is perfectly constant for $z > 0.5w$. This confirms that the increase of the area of the liquid-air interface has no impact on the evaporation from the sample. This effect results from the fact that the vapor density mainly varies over an entrance length of the order of the channel width, leading to a rapid decrease of the contribution to the drying rate from the liquid-air interface situated at larger distance from the entrance. More precisely $F(x)$ decreases exponentially

with x and $F(x=w) \approx 10^{-3} F(0)$ for both geometries.

This result also implies that the thickness of the liquid films beyond the entrance length has no impact on the drying rate. Since our experimental data show a strong decrease of the drying rate in a regime where the film thickness decreases this suggests that this is the shape of the interface around the channel entrance which plays a critical role on the drying rate.

In order to test this idea we looked at the impact of the geometry when the film thickness (h) decreases. The exact shape of the air/water interface is not measured with enough accuracy in our experiments, so to model the variety of evolution we consider three scenarios based on parameter h for the entrance shape of the interface, which cover the various trends that can be expected for the evolution of this shape (see Figure 3): in (C) the angle between the interface and the channel axis is fixed at 45°; in (D) the distance of transition is maintained to h_0, which implies to decrease the angle; in (E) this is the length of the transition region which is kept constant. We then represent the scaled drying rate as a function of the saturation (see Figure 5), i.e. the ratio of the area of the liquid region to the whole area of the geometry.
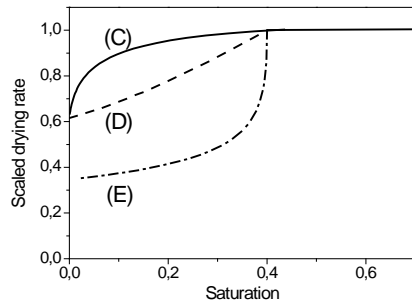
Figure 5: Scaled drying rate as a function of the saturation for our simulations (black) with different shapes of the entrance interface in the period of decreasing film thickness.

In all three configurations, the drying rate decreases when h decreases, i.e. when the saturation decreases, but the exact kinetics varies drastically with the shape of the liquid-air interface at the entrance. In fact the main characteristics changing from (C) to (E) is the slope (α) of the interface from the entrance: we have $\alpha = 45°$ for (C), $\tan \alpha = h/h_0$ for (D) and $\tan \alpha = \left((h_0/h)^2 - 1 \right)^{-1/2}$. This in particular implies that the distance of junction between the slope and the constant thickness region is farther from (C) to (E), and finally the area of the interface in this region is smaller. This qualitately explains that the drying rate decreases faster from (C) to (E) since we have seen that the vapor flux decreases with the distance from the free surface of the sample.

CONCLUSIONS

These results can be extrapolated to more complex (real) porous media. When capillary effects are dominant, if wet patches are sparse, the evolution of the exact shape of the liquid/air interface will govern the evaporation rate. Even with the same porosity a slight variation in pore shape, in particular close the free surface of the sample, can induce variations of the drying rate by orders of magnitude. Thus there may exist situation in which there is no receding front in the Falling Rate Period.

REFERENCES
[1] Chauvet F, Duru P, Geoffroy S, Prat M (2009) Three periods of drying of a single square capillary tube. Phys. Rev. Lett. 103, 124502

[2] Coussot P (2000) Scaling approach of the convective drying of a porous medium. Eur. Phys. J. B 15, 557.

[3] Faure P and Coussot P (2010) Drying of a model soil. Phys. Rev. E 82, 036303.

[4] Gonçales TD, Pel L, Rodrigues JD (2009) Influence of paints on drying and salt distribution processes in porous building materials. Constr. and Build. Mat. 23, 1751-1759

[5] Keita E, Faure P, Rodts S and Coussot P (2013) MRI evidence for a receding-front effect in drying porous media. Phys. Rev. E 87, 062303.

[6] Li J, Cabane B, Sztucki M, Gummel J and Goehring L (2012) Drying dip-coated colloidal films. Langmuir 28, 200.

[7] Shokri N and Or D (2011) What determines drying rates at the onset of diffusion controlled stage-2 evaporation from porous media? Water Res. Res. 47, W09513

[8] Yiotis AG, Boudouvis AG, Stubos AK, Tsimpanogiannis IN, and Yortsos Y C (2003) Effect of liquid films on the isothermal drying of porous media. Phys. Rev. E 68, 037303.